ELSEVIER

Contents lists available at ScienceDirect

Harmful Algae

journal homepage: www.elsevier.com/locate/hal





Pelagic Sargassum in the Gulf of Mexico driven by ocean currents and eddies

Yingjun Zhang ^a, Chuanmin Hu ^{a,*}, Dennis J. McGillicuddy Jr. ^b, Brian B. Barnes ^a, Yonggang Liu ^a, Vassiliki H. Kourafalou ^c, Shuai Zhang ^a, Frank J. Hernandez ^d

- ^a College of Marine Science, University of South Florida, St. Petersburg, FL, United States
- ^b Department of Applied Ocean Physics and Engineering, Woods Hole Oceanographic Institution, Woods Hole, MA, United States
- c Rosenstiel School of Marine and Atmospheric Science, University of Miami, Miami, FL, United States
- ^d Southeast Fisheries Science Center, National Marine Fisheries Service, NOAA, Pascagoula, MS, United States

ARTICLE INFO

Edited by: Dr. C. Gobler

Keywords: Sargassum Gulf of Mexico Caribbean Sea Loop Current System Ocean currents Satellite observation

ABSTRACT

Pelagic Sargassum in the Gulf of Mexico (GoM) plays an important role in ocean biology and ecology, yet our knowledge of its origins and transport pathways is limited. Here, using satellite observations of Sargassum areal density and ocean surface currents between 2000 and 2023, we show that large amounts of Sargassum in the GoM can either originate from the northwestern GoM or be a result of physical transport from the northwestern Caribbean Sea, both with specific transport pathways. Sargassum of the northwestern GoM can be transported to the eastern GoM by ocean currents and eddies, eventually entering the Sargasso Sea. Sargassum entering the GoM from the northwestern Caribbean Sea can be transported in three different directions, with the northward and eastward transports governed by the Loop Current System (LCS) and westward transport driven by the westward extension of the LCS, the propagation or relaying of ocean eddies, the wind-driven westward currents on the Campeche Bank with or without eddies, and the westward currents with/without currents associated with eddies in the northern/central GoM. Overall, the spatial distribution patterns of pelagic Sargassum in the GoM are strongly influenced by the LCS and relevant eddies.

1. Introduction

The Gulf of Mexico (GoM, Fig. 1a) is characterized by a wide range of habitats and relatively high biodiversity (e.g., Chen, 2017), with over 15,000 recorded species representing over 40 phyla (Felder et al., 2009). Among the most speciose communities are those associated with holopelagic Sargassum (S. natans and S. fluitans) macroalgae (Gower et al., 2006; Gower and King, 2011, 2020; Doyle and Franks, 2015; Hu et al., 2016a, 2016b; Siuda et al., 2016; Martin et al., 2021; Fig. 1b). These seaweeds provide essential habitat and food sources for marine animals such as crabs, fish, shrimps, turtles, and sea birds (Wells and Rooker, 2004; Casazza and Ross, 2008; Witherington et al., 2012; Sanchez-Rubio et al., 2018). In addition, Sargassum may have far-reaching impacts on nutrient remineralization and primary productivity (Hu et al., 2021; Lapointe et al., 2021; McGillicuddy et al., 2023), as well as the potential to serve as raw materials for the production of biofuels and pharmaceutical products (Milledge et al., 2016; Amador-Castro et al., 2021; Orozco-González et al., 2022). In spite of these potential benefits, large Sargassum beaching events can have deleterious effects on human

health, local tourism and economies, and coastal ecosystems (e.g., Smetacek and Zingone, 2013; Webster and Linton, 2013; Siuda et al., 2016; Van Tussenbroek et al., 2017; Gower and King, 2019).

To date, our understanding of the origins and transport pathways affecting the spatial distributions of GoM Sargassum is limited. Based on the sequential monthly maps of Sargassum population in the GoM and north Atlantic Ocean, derived from Medium Resolution Imaging Spectrometer (MERIS) satellite measurements between 2002 and 2008, Gower and King (2011) showed that Sargassum developed locally in the northwestern GoM in spring, and was then transported to the southeastern GoM and north Atlantic Ocean in summer and fall through major ocean currents such as the Loop Current (LC), Florida Current (FC), and Gulf Stream (see the schematic diagram of these ocean currents in Fig. 1a). More recent satellite observations suggest a new source region in the tropical Atlantic (e.g., Gower et al., 2013; Wang and Hu, 2017; Wang et al., 2019; Gower and King, 2020), which could deliver large amounts of Sargassum to the GoM. Satellite imagery from the Sargassum Watch System (SaWS, Hu et al., 2016b; https://optics.marine.usf.edu/ projects/saws.html) revealed that Sargassum in the Caribbean Sea could be transported to the GoM, yet it is unclear how the transport of

^{*} Corresponding author at: College of Marine Science, University of South Florida, 140 7th Ave. South, St. Petersburg, FL 33701, United States. E-mail address: huc@usf.edu (C. Hu).

Notations

FC Florida Current

GASB Great Atlantic Sargassum Belt

GoM Gulf of Mexico
LC Loop Current
LCE Loop Current Eddy
LCS Loop Current System

MERIS Medium Resolution Imaging Spectrometer
MODIS Moderate Resolution Imaging Spectroradiometer

OLCI Ocean and Land Colour Imager SaWS Sargassum Watch System

Sargassum within the GoM is influenced by major ocean currents and eddies.

The objectives of this study are to explore the origins of *Sargassum* in the GoM and to investigate the mechanisms impacting the transport and spatial distributions of GoM *Sargassum*. This is achieved through analyzing the satellite-derived *Sargassum* distributions in the context of ocean surface currents and eddies.

2. Data and methods

Weekly $0.1^{\circ} \times 0.1^{\circ}$ Sargassum areal density maps from February 2000 to June 2023 were derived from daily Moderate Resolution Imaging Spectroradiometer (MODIS) measurements (from both Terra and Aqua satellites) using the method described in Wang and Hu (2016), with images available through the SaWS (Hu et al., 2016b; https://opti cs.marine.usf.edu/projects/saws.html). Briefly, each image pixel (about 1 km in size) during a week within a grid was classified to be either Sargassum containing, Sargassum free, or invalid (due to either clouds, sun glint, straylight, or other factors). This determination was based on an algorithm to quantify the pixel's "red-edge" reflectance (i.e., enhanced reflectance in the near infrared wavelengths; Wang and Hu, 2016) and specific image processing methods to remove noise. The spectral shapes of some randomly selected Sargassum-containing pixels were inspected to confirm presence of Sargassum instead of other floating matters (e.g., Trichodesmium), spectra-differencing technique demonstrated by Qi et al. (2020). Basically, for MODIS, the difference spectra between the Sargassum-containing pixel and nearby water pixel showed elevated reflectance around 645 nm without the spectral "wiggling" features in the blue-green wavelengths due to pigments specific to Trichodesmium (Hu et al., 2010). For the Ocean Colour and Land Imager (OLCI), similar elevated reflectance was observed around 620 nm for both Sargassum and Trichodesmiumm pixels, but the latter showed relatively higher reflectance at 510 nm than the former (Qi et al., 2020). Once the randomly selected pixels were confirmed to be dominated by Sargassum, all classified image features were assumed to contain Sargassum.

Each Sargassum-containing pixel was quantified for its areal density (0 %–100 %) using lower and upper bound threshold values established through field measurements and image statistics. The mean areal density for a grid within a week was defined as the arithmetic mean of all Sargassum-containing and Sargassum-free pixels, with each pixel contributing 0 %–100 %. Because the areal density is proportional to biomass density with a mean conversion factor of 3.34 kg wet biomass m^{-2} (Wang et al., 2018), the areal density and biomass density are used interchangeably in this study.

Daily $0.25^{\circ} \times 0.25^{\circ}$ altimetry-based ocean surface geostrophic current data between February 2000 and June 2023, provided by the Copernicus Marine Environment Monitoring Service (CMEMS, https://marine.copernicus.eu/), were used to analyze the spatial distributions and temporal variability of ocean surface currents and

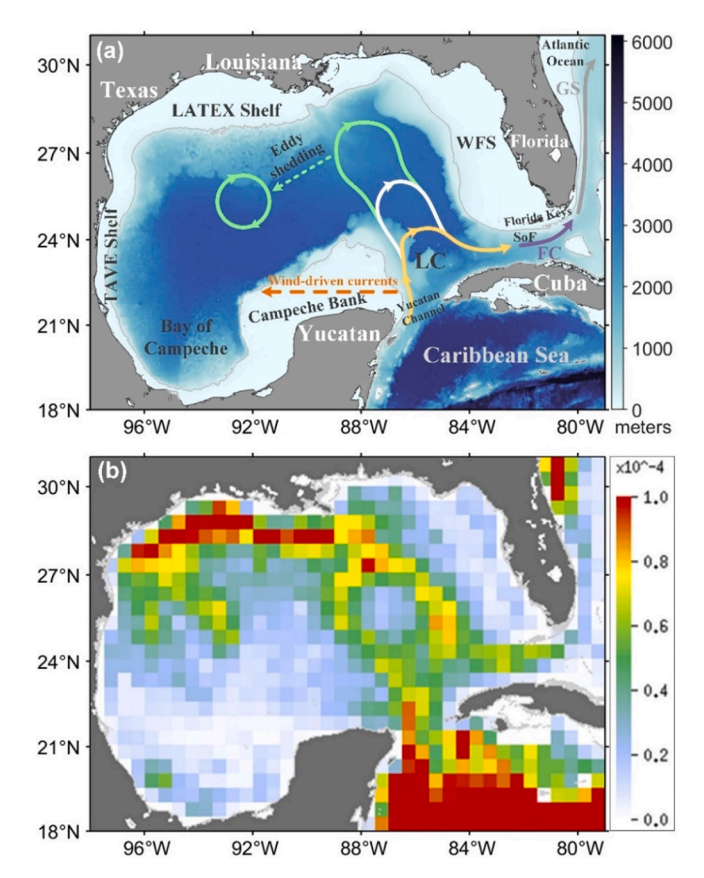


Fig. 1. (a) Bathymetry of the Gulf of Mexico and the northwestern Caribbean Sea. The thin gray lines denote the 200 m isobath. Important geographic features are also noted: Yucatan Channel, Straits of Florida (SoF), Florida Keys, West Florida Shelf (WFS), Louisiana-Texas (LATEX) Shelf, Tamaulipas-Veracruz (TAVE) Shelf, Bay of Campeche, Campeche Bank, and the Atlantic Ocean. The Florida Current (FC) and Gulf Stream (GS) are indicated by thick purple and gray curves with arrows, respectively. The dashed orange line with an arrow on the Campeche Bank denotes the ocean currents driven by northeasterly or easterly winds throughout the year (e.g., Zavala-Hidalgo et al., 2014; Zhang and Hu, 2021). The yellow, white, and green curves with arrows individually denote the Loop Current (LC) extension in three different stages (i. e., "port-to-port", "averagely extended", and "fully extended"), during which it has a northward extension at ~24, 26, and 28°N, respectively (Leben, 2005). After extending northward from ~24°N to ~28°N, a large anticyclonic LC Eddy (LCE, green circle) may form and detach from the extended LC. Before its final separation from the LC, the LCE may re-attach to, and detach from the LC several times (Leben, 2005; Schmitz, 2005). After the separation from the LC, LCEs predominantly propagate westward at speeds of ~2-5 km/day (Elliott, 1982; Hamilton et al., 1999). (b) Distribution of mean Sargassum areal density during April-September of 2011-2020, with a grid size of 0.5°. Color codes denote fractional cover (e.g., $1 \times 10^{-4} = 0.01$ %). Note that the weekly Sargassum areal density images used in this study have a grid size of 0.1°.

mesoscale eddies in the GoM. This product provides an important source of observations for surface ocean circulation studies (Vignudelli et al., 2006). It has global coverage, but only data for the GoM were used here. In addition, data before August 2021 are in delayed-time mode, while the data are in near-real-time mode thereafter. This product has been widely used in previous GoM ocean circulation studies and other relevant studies (e.g., Alvera-Azcarate et al., 2009; Liu et al., 2014, 2016; Weisberg et al., 2016; Zhu and Liang, 2020; Zhang et al., 2022b; Zhang et al., 2023). Daily data were averaged to generate weekly maps to match the time frame of *Sargassum* maps.

3. Results

The distribution map of mean Sargassum areal density during

April–September of 2011–2020 (Fig. 1b), shows *Sargassum* nearly everywhere in the GoM, with more *Sargassum* in the northwestern GoM and along the LC edges than in other locations. Such a distribution can be explained in the context of ocean circulation patterns and their variations. Examination of the combined *Sargassum* areal density and ocean current maps revealed multiple pathways of *Sargassum* transport that affected *Sargassum* distributions in the GoM. These pathways are broadly characterized into two categories: 1) local *Sargassum* origin (i.e., from within the GoM) and 2) remote *Sargassum* origin (i.e., from outside the GoM), and they are schematically illustrated in Fig. 2.

The first category (local origin in the northwestern GoM) has already been discussed by Gower and King (2011), where sequential monthly maps of *Sargassum* population in the GoM and north Atlantic Ocean,

derived from MERIS satellite observations during 2002–2008, were used to infer the eastward transport of *Sargassum* via the LC and FC. Here, the image sequence in Fig. 3 clearly shows the progression of the eastward movement of *Sargassum* during May and June 2014. The continuous evolution of *Sargassum*'s eastward movement within the GoM can also be seen from an animation provided in the Supporting Information. The year of 2014 was selected here because this is the year during which large amounts of *Sargassum* were first found in the northwestern GoM between May and early June (Figs. 3a–3c), while the eastern GoM showed limited amounts and the northwestern Caribbean Sea showed nearly no *Sargassum*. During this period, *Sargassum* biomass density in the area north of the Loop Current System (LCS; box 2 in Fig. 3) increased over time. By mid–late June, *Sargassum* amount on the West

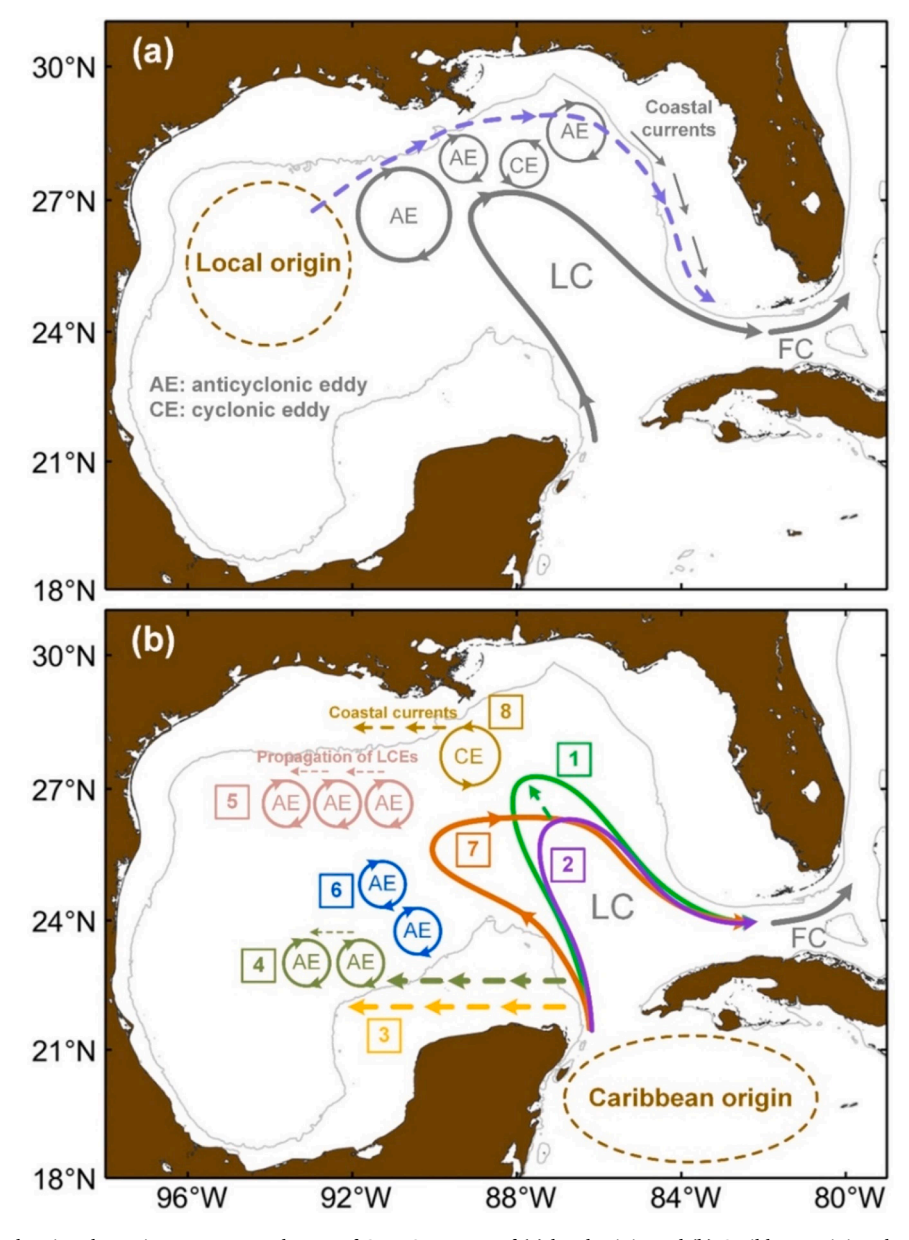


Fig. 2. Schematic diagrams showing the major transport pathways of GoM Sargassum of (a) local origin and (b) Caribbean origin. The thin gray lines in each figure denote the 200 m isobath. LC and FC represent the Loop Current and Florida Current, respectively. The dashed blue curves with arrows in (a) indicate the eastward transport pathway of Sargassum of local origin, associated with ocean eddies in the northern GoM and the southeastward coastal currents on the West Florida Shelf. Sargassum transport pathways shown in (b) are listed as follows. 1: northward transport by the northward intrusion of the Loop Current extension; 2: eastward transport by the direct eastward transport of the Loop Current; 3: westward transport by the wind-driven ocean currents on the Campeche Bank; 4: westward transport by the wind-driven ocean currents on the Campeche Bank and eddies; 5: westward transport by the westward propagation of eddies (e.g., Loop Current Eddies or LCEs); 6: westward transport by the relaying of eddies (e.g., LCEs); 7: westward transport by the westward extension of the Loop Current System; 8: westward transport by the westward currents (e.g., coastal currents on the Louisiana–Texas Shelf) with/without eddies in the northern/central GoM.

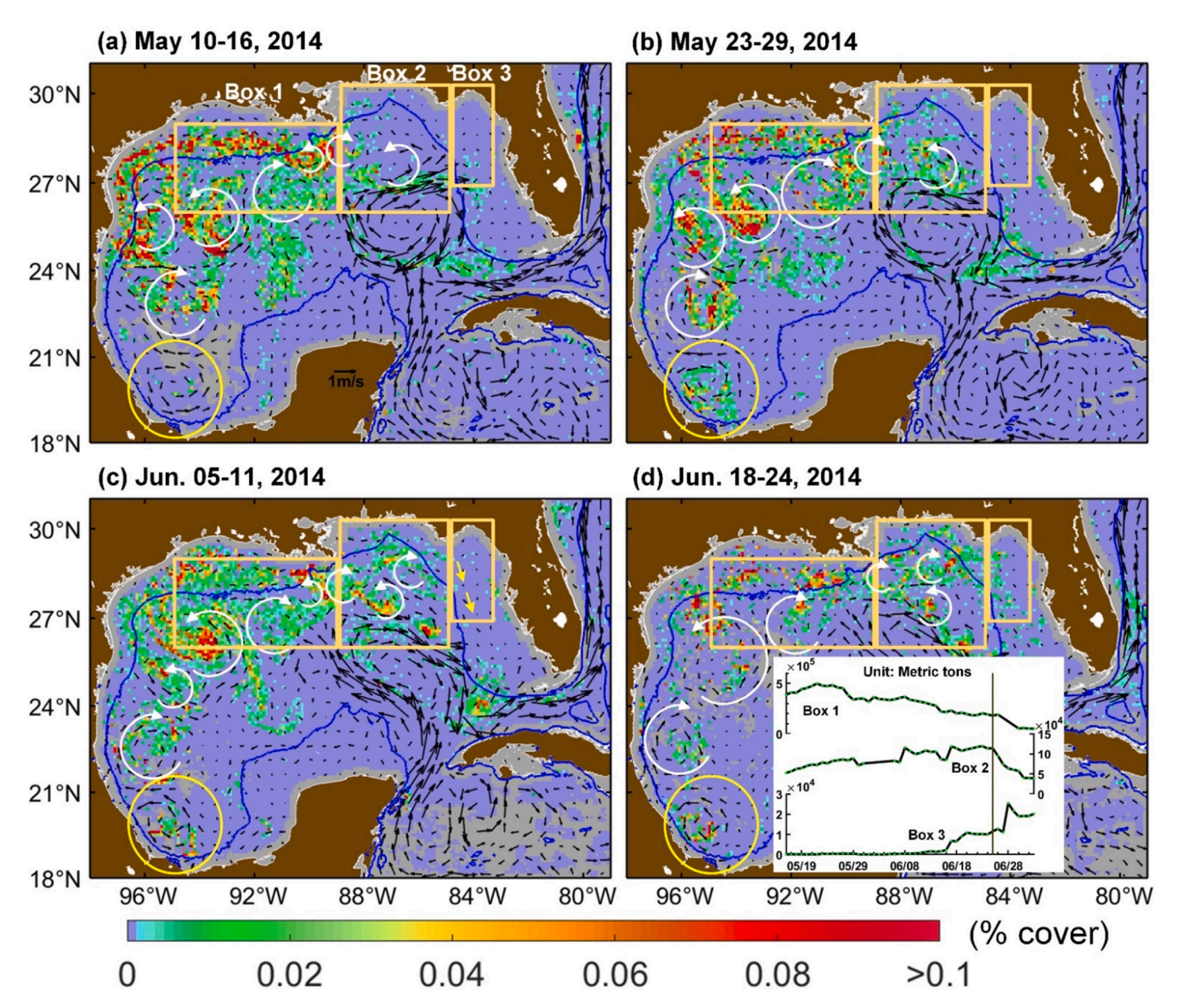


Fig. 3. Distributions of MODIS weekly *Sargassum* areal density in the GoM during May and June 2014, showing the eastward transport of *Sargassum* from the northwestern GoM to the eastern GoM. A value of 0.02 on the color bar denotes 0.02 %. Gray color indicates no data, and the blue lines represent the 200 m isobath in each figure. Three areas annotated with yellow boxes in each figure were chosen for the time series analysis of *Sargassum* biomass density, and the corresponding results are presented in the inset figure of (d). Note that several consecutive dates (i.e., June 27–29 for box 1 and June 1–5 for box 2) had relatively large cloud cover, thus *Sargassum* biomass density data for these dates over box 1 or box 2 were excluded from the time series analysis. The yellow circle in each figure highlights a cyclonic eddy in the Bay of Campeche. The black vectors (with scale overlaid on land in (a)) represent altimetry-based ocean surface currents in each figure, and the white curves with arrows indicate the eddies located in the western and northern GoM, determined from visual inspections.

Florida Shelf also increased (box 3 in Fig. 3). The combined *Sargassum* and ocean surface current maps prior to spring 2014 revealed nearly no *Sargassum* in the Caribbean Sea between November 2012 and May 2014 (figures not shown here), suggesting that the large amounts of *Sargassum* in the northwestern GoM appear to have originated from the northwestern GoM interior, and then been transported to the eastern GoM and eventually to the north Atlantic Ocean. Such observations confirm the hypothesis proposed by Gower and King (2011).

In the 2014 case, the transport of *Sargassum* from the northwestern GoM to the eastern GoM was mainly driven by ocean currents and eddies, as schematically shown in Fig. 2a. Specifically, the anticyclonic eddies and eastward currents inside box 1 of Fig. 3 helped transport *Sargassum* from west to east, and the LC, anticyclonic eddies, and other eastward currents in box 2 of Fig. 3 also facilitated the eastward transport of *Sargassum*. After reaching the eastern boundary of box 2, *Sargassum* was further transported southeastward on the West Florida

Shelf through the southeastward currents (annotated with yellow arrows in box 3 of Fig. 3c). On the other hand, a portion of Sargassum near the southern boundary of box 2 has been transported southeastward by the LC to the Straits of Florida. The distributions of these surface currents and eddies, as well as the changes of Sargassum biomass density can be clearly visualized in an animation provided in the Supporting Information. Note that the southeastward currents on the West Florida Shelf and the currents associated with the two anticyclonic eddies in box 2 of Figs. 3c-3d had speeds of \sim 20–30 cm/s. In addition to the influence of ocean currents and eddies, the changes of wind direction from easterly to westerly or southwesterly (Le Hénaff and Kourafalou, 2016) may also have contributed to the eastward transport of Sargassum. A time series analysis was conducted to further understand the eastward transport of Sargassum within the GoM. Specifically, the time series of Sargassum biomass density over boxes 1-3 from May 16 to July 3, 2014, was derived from weekly running mean Sargassum areal density maps,

and the results are presented in the inset figure of Fig. 3d. It is clear that box 1 was characterized by decreasing *Sargassum* biomass density, while box 2 was characterized by increasing biomass density until June 25 (annotated with a black vertical line in the inset figure), after which *Sargassum* biomass density decreased gradually. Regarding box 3, *Sargassum* biomass density increased sharply from June 16 to June 28. These results clearly demonstrate the eastward transport of *Sargassum* from west to east over the northern GoM.

The second category has not been described before in the refereed literature. In this pathway, *Sargassum* in the GoM has a remote origin in the tropical Atlantic Ocean where the Great Atlantic *Sargassum* Belt (GASB) forms nearly every spring–summer since 2011 (Gower et al., 2013; Wang et al., 2019; Gower and King, 2020). Specifically, large amounts of *Sargassum* were first observed in the tropical Atlantic Ocean during early spring, which were then transported to the Caribbean Sea via dominant ocean currents and eddies (Andrade-Canto et al., 2022),

and eventually to the GoM from the Caribbean Sea. A similar transport mechanism was reported for satellite-tracked drifters launched in the eastern Caribbean Sea (Richardson, 2005) and the central Atlantic Ocean (Franks et al., 2016; Van Sebille et al., 2021; Drouin et al., 2022). Fig. 4 clearly shows that *Sargassum* in the northwestern Caribbean Sea is transported into the GoM by surface currents.

Upon entering the GoM, *Sargassum* can reach the central, western, northern, and southeastern GoM, as well as the Straits of Florida and even the east coast of Florida, all driven by ocean currents and eddies (as schematically shown in Fig. 2b). The LCS and eddies exhibit complicated spatial patterns within the GoM and the pattern evolution has variability on different time scales (e.g., Leben, 2005; Schmitz, 2005; Liu et al., 2016). The individual panels in Fig. 4 illustrate how the different transport pathways evolved in time, all controlled by the LCS, wind-driven ocean currents on the Campeche Bank, ocean currents in the northern/central GoM, and relevant eddies. These include the

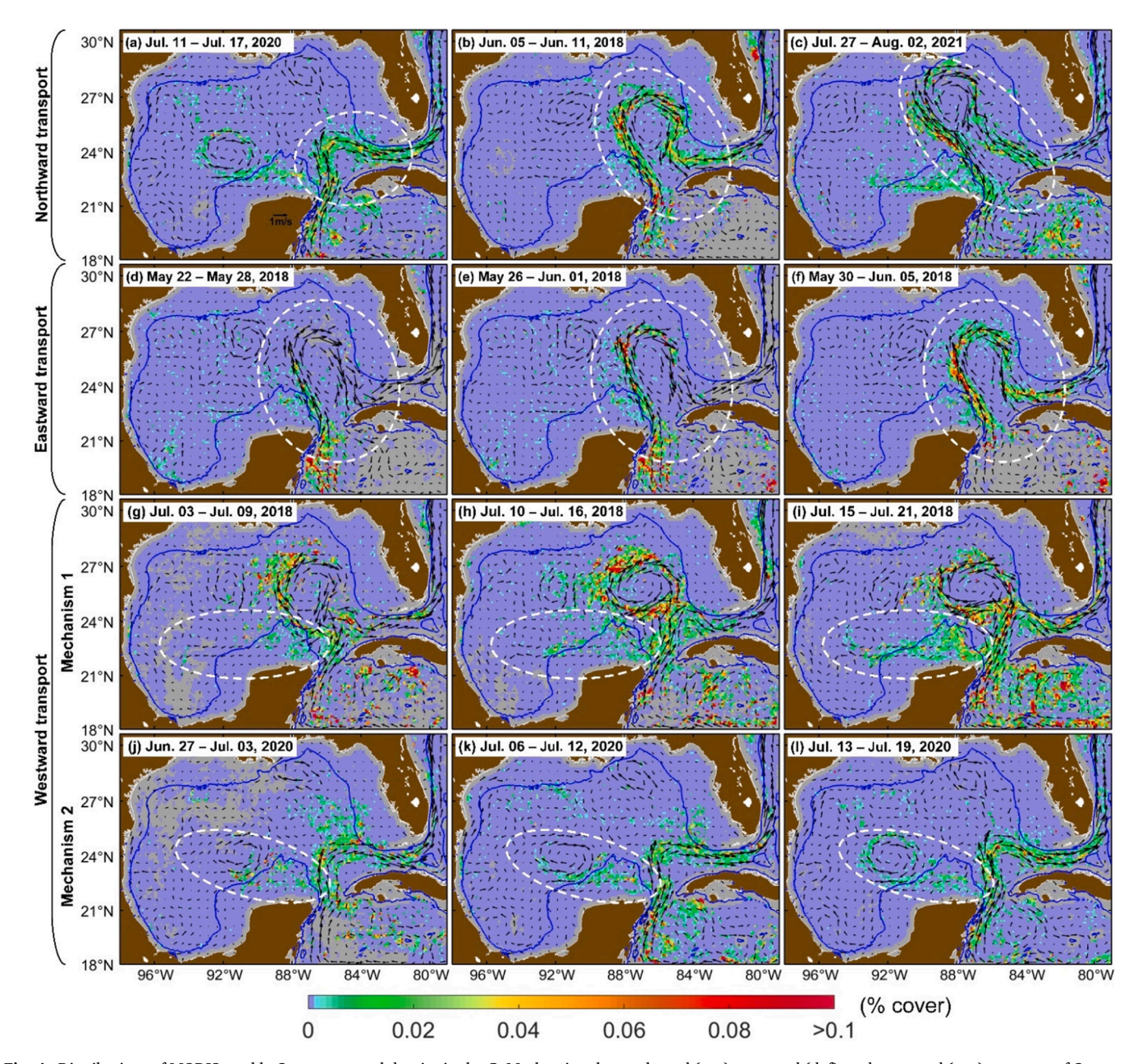


Fig. 4. Distributions of MODIS weekly *Sargassum* areal density in the GoM, showing the northward (a–c), eastward (d–f), and westward (g–x) transport of *Sargassum* of Caribbean origin. A value of 0.02 on the color bar denotes 0.02 %. Gray color indicates no data, and the blue lines represent the 200 m isobath in each figure. The dashed white ellipse in each figure highlights the *Sargassum* patterns under physical transport. The black vectors in each figure (with scale shown in (a) and (m)) represent altimetry-based ocean surface currents. Note that dates in (a)–(c) are not sequential.

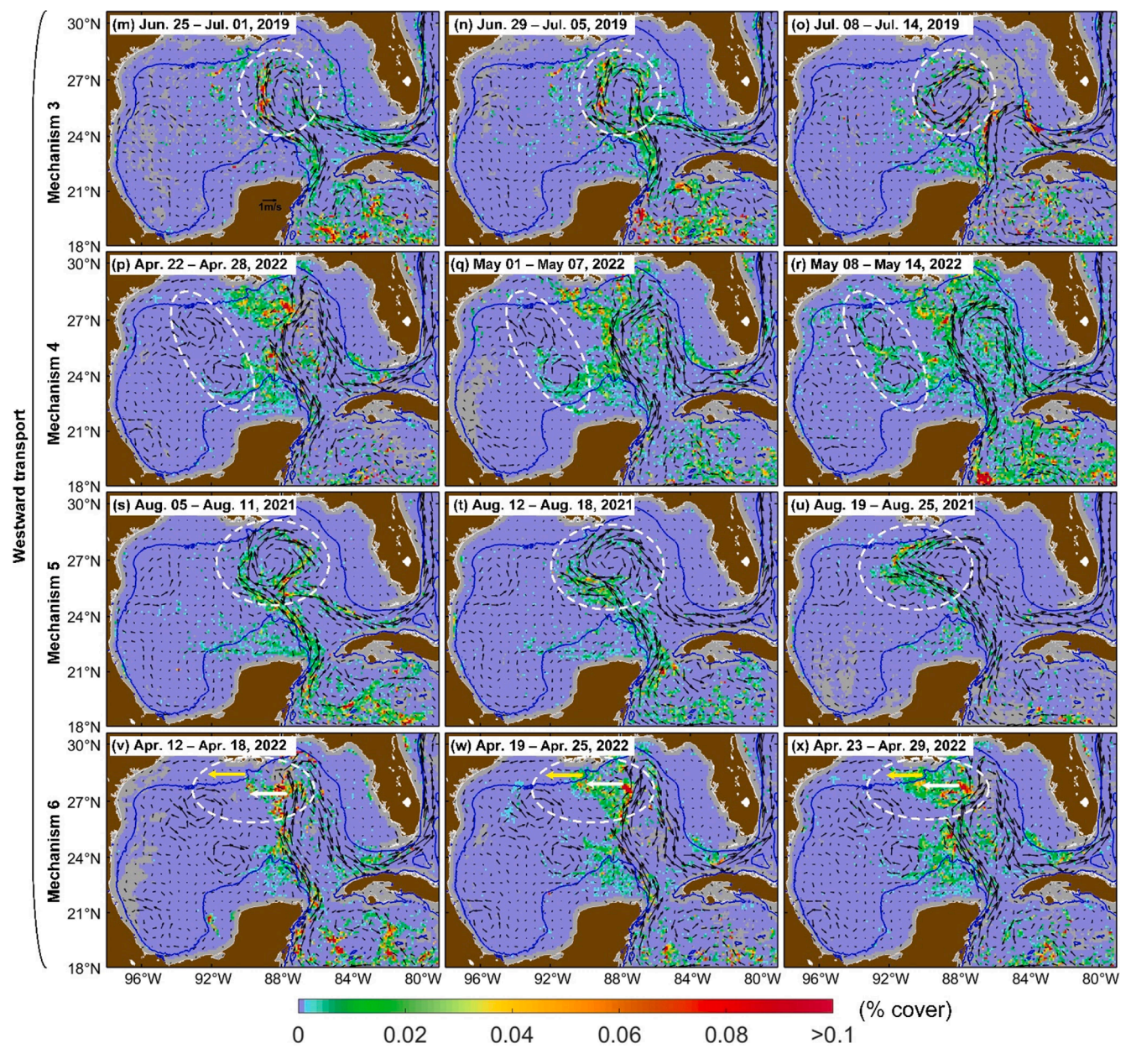


Fig. 4. (continued).

northward transport (Fig. 4a-c), eastward transport (Fig. 4d-f), and westward transport (Fig. 4g-x).

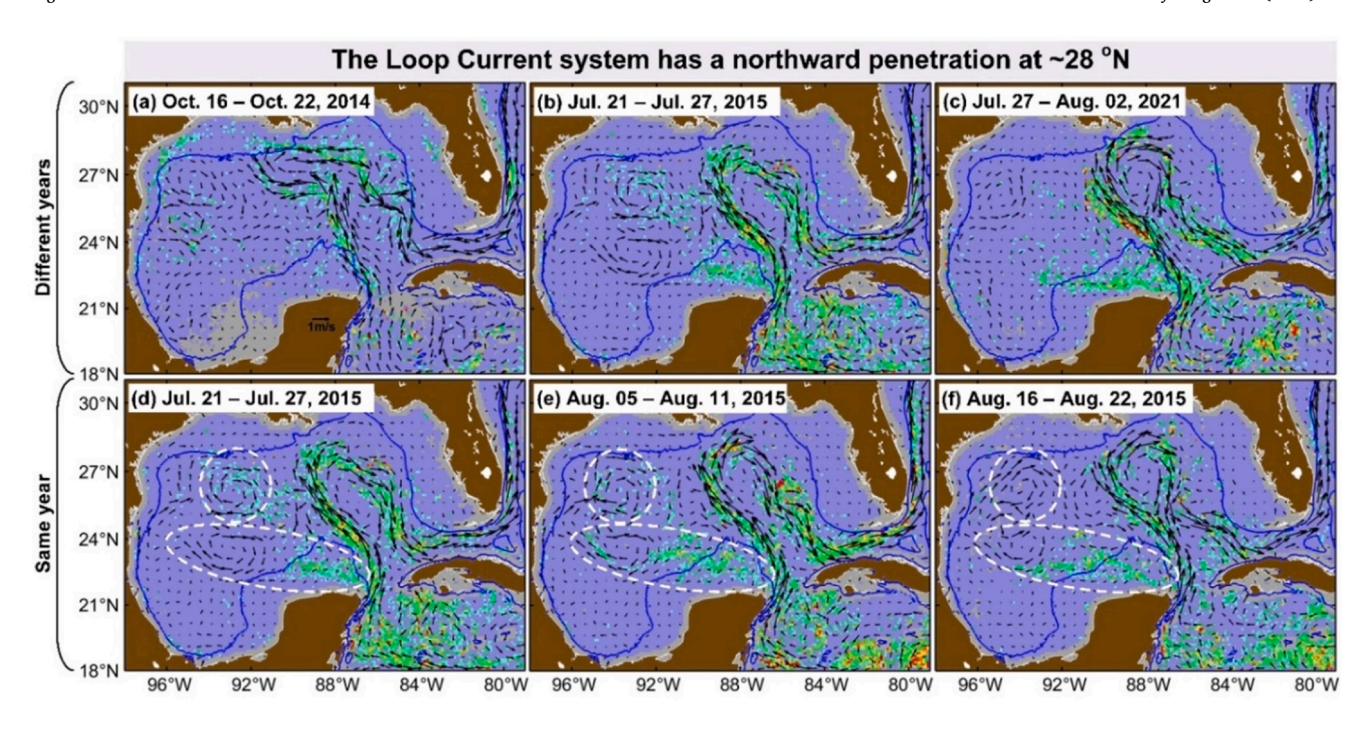
The northward transport of *Sargassum* is illustrated in Fig. 4a–c (corresponds to pathway #1 in Fig. 2b), where the positions of *Sargassum* at ~24, 26, and 28°N correspond exactly to the three typical stages of the LC extension, including the "port-to-port", "averagely extended", and "fully extended" stages (shown as yellow, white, and green curves with arrows in Fig. 1a, respectively; Leben, 2005).

The eastward transport of *Sargassum* is shown in Fig. 4d–f (corresponds to pathway #2 in Fig. 2b). During May 22–28, 2018, *Sargassum* appeared in the western branch of the LC. Four days later, *Sargassum* appeared in the eastern branch of the LC, and then was transported to the Straits of Florida during May 30–June 5, which finally reached the north Atlantic Ocean along the east coast of Florida.

The westward transport of *Sargassum* is more complex (Fig. 4g–x), which can be characterized by the following six mechanisms:

- (1) Westward transport of the wind-driven ocean currents on the Campeche Bank (pathway #3 in Figs. 2b and 4g-i)
- (2) Westward transport of the wind-driven ocean currents on the Campeche Bank and eddies (e.g., LC Eddies or LCEs; pathway #4 in Figs. 2b and 4j–l, 5d–e)
- (3) Westward propagation of eddies (e.g., LCEs; pathway #5 in Figs. 2b and 4m-o, 5d-e)
- (4) Relaying of eddies (pathway #6 in Figs. 2b and 4p-r)
- (5) Westward extension of the LCS (pathway #7 in Figs. 2b and 4s-u)
- (6) Westward transport of the westward currents with/without currents associated with eddies in the northern/central GoM (pathway #8 in Figs. 2b and 4v-x)

As illustrated in Fig. 4g-i, once *Sargassum* enters the GoM from the northwestern Caribbean Sea through the Yucatan Channel, the westward transport of the wind-driven ocean currents on the Campeche Bank (with schematic diagram shown in Figs. 1a and 2b) can bring *Sargassum* from the east to the west directly. On the other hand, if *Sargassum*



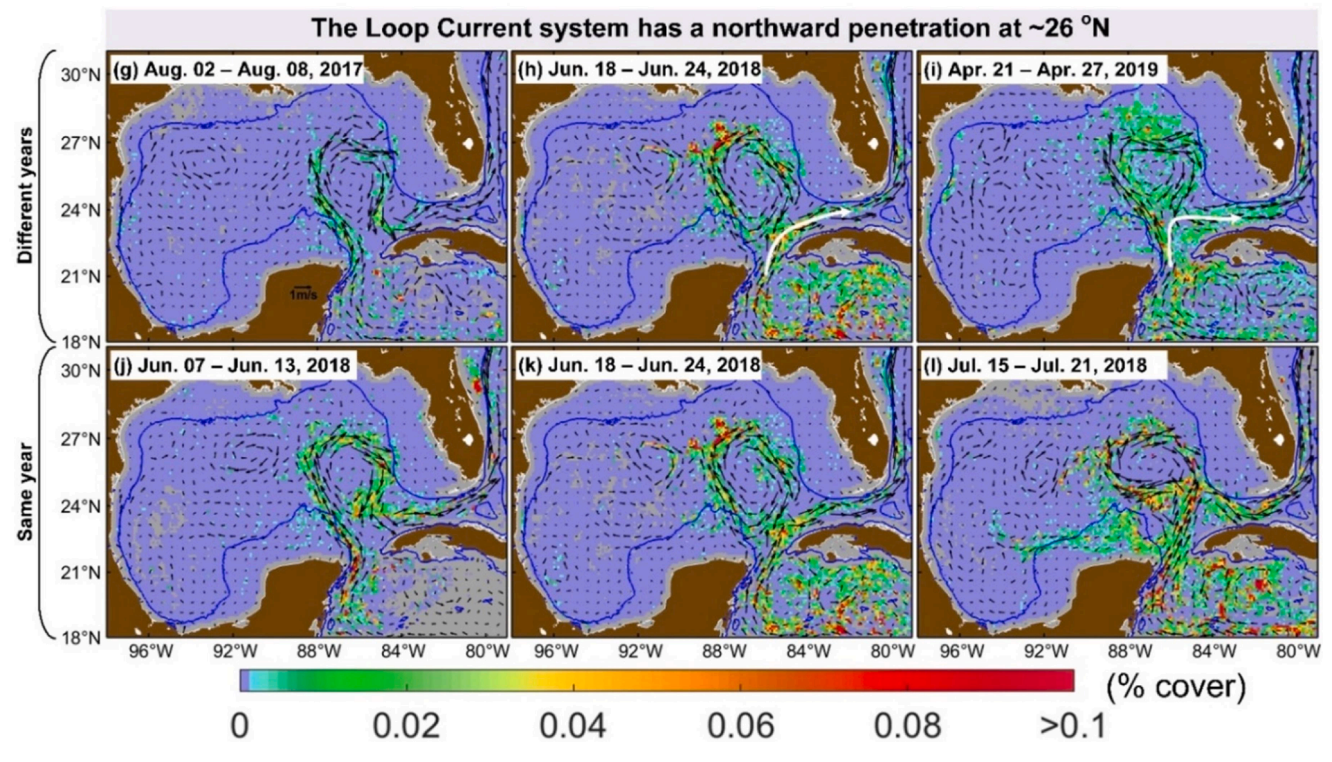


Fig. 5. Distributions of MODIS weekly Sargassum areal density in the GoM, showing the different spatial patterns of Sargassum when the LCS has a northward penetration at \sim 28°N (a–f) and \sim 26°N (g–l). For the first case (northward penetration at \sim 28°N), the Sargassum distribution maps are differentiated into different years (a–c) and the same year (d–f). For the other case (northward penetration at \sim 26°N), (g–i) and (j–l) show the spatial patterns of Sargassum in different years and the same year, respectively. A value of 0.02 on the color bar denotes 0.02 %. Gray color indicates no data, and the blue lines represent the 200 m isobath in each figure. The black vectors in each figure (with scale shown in (a) and (g)) represent altimetry-based ocean surface currents. The dashed white circles and ellipses in (d)–(f) highlight two examples of westward transport of Sargassum. The white curves with arrows in (h) and (i) indicate the direct transport of Sargassum from the northwestern Caribbean Sea to the Straits of Florida.

encounters eddies (e.g., LCEs) during its westward transport driven by the wind-driven ocean currents on the Campeche Bank, the eddies can further transport *Sargassum* westward (Figs. 4j–l and 5d–e). The third mechanism explaining the westward movement of *Sargassum* is shown in Figs. 4m–o and 5d–e. Specifically, the westward propagation of eddies

(e.g., LCEs; annotated with white circles in Figs. 4m-o and 5d-e) allowed the westward transport of *Sargassum*, where *Sargassum* was mostly on the eddy edge rather than in the eddy center. Likewise, the relaying between eddies (e.g., LCEs) can allow *Sargassum* to be transported both westward and northward, as is clearly shown in Fig. 4p-r

and an animation provided in the Supporting Information.

After getting to the northern/northwestern edge of the LCS, the westward transport of Sargassum can be achieved through the westward extension of the LCS. As shown in Fig. 4s-u, during August 5-11, 2021, Sargassum appeared on the western edge of the LCE at ~90°W, and then reached ~92°W after two weeks (Fig. 4u). The direct westward extension of the LCS within the two weeks facilitated the westward transport of Sargassum. Additionally, the westward transport of the westward currents with/without currents associated with eddies in the northern/ central GoM can also transport Sargassum westward. According to Fig. 4v, the westward currents (annotated with white arrows in Fig. 4v–x) moved *Sargassum* from the LCS to ~90°W in mid-April 2022. These currents were the northern part of a cyclonic eddy and the southern part of an anticyclonic eddy (see clear pictures in an animation provided in the Supporting Information). In around one week, the cyclonic eddy entrained more Sargassum and lots of Sargassum was transported onto the Louisiana-Texas Shelf (Fig. 4w), and then Sargassum was transported further westward under the influence of the westward coastal currents (annotated with yellow arrows in Fig. 4v-x) on the Louisiana-Texas Shelf in late April 2022 (Fig. 4x).

The durations (number of days) of the aforementioned transport mechanisms of Sargassum of Caribbean origin are summarized in Table 1 for the years after 2013, during which apparent transport pathways of large amounts of Sargassum in the GoM have been observed in most years. It was found that each of the Sargassum transport mechanisms exhibited strong interannual variability, and that most of them lasted longer in major Sargassum years (e.g., 2018, 2019, 2021, and 2022) than in other years. In addition, among the six mechanisms of westward transport of Sargassum, the mechanisms involving the westward transport of the wind-driven ocean currents on the Campeche Bank with/ without eddies, westward propagation of eddies, and the westward extension of the LCS play a more important role in the westward transport of GoM Sargassum compared to the other two (i.e., relaying of eddies; westward transport of the westward currents with/without currents associated with eddies in the northern/central GoM). It is worth mentioning that Sargassum transport mechanisms falling under the second category (remote origin in the tropical Atlantic Ocean) may occur concurrently. For instance, during the northward intrusion of the LC, Sargassum coming from the Caribbean Sea can be transported both northward and eastward by the LC in the GoM. In addition, a transition from one mechanism to another may occur gradually as the dynamic LCS evolves in time. Similarly, the transport of GoM Sargassum under the second category may also occur concurrently with the transport of Sargassum under the first category (i.e., local origin in the northwestern GoM).

The image sequences above clearly revealed the transport pathways of the observed large amounts of <code>Sargassum</code> in the GoM and the effects of the LCS on the <code>Sargassum</code> transport. Indeed, the LCS not only plays a key role in the northward, westward, and eastward transport of <code>Sargassum</code>, but can also regulate the spatial distribution patterns of <code>Sargassum</code>. On

the other hand, even for the same physical mechanism of Sargassum transport (via the LCS) as shown above, the inter-annual variability of the LCS can lead to different Sargassum distribution patterns. For example, when the main axis of the LCS had a northward penetration at ~28°N (Fig. 5a-c), the spatial patterns of the LCS differed substantially in three different years (i.e., 2014, 2015, and 2021), as did the corresponding distribution patterns of Sargassum. A similar case can occur even within the same year (e.g., 2015), as demonstrated in Fig. 5d-f. During the period of late July-late August 2015, Sargassum was transported westward by the westward movement of a LCE (white circles in Fig. 5d-f) and the westward transport of the wind-driven ocean currents on the Campeche Bank (white ellipses in Fig. 5d-f). The LCE-transported Sargassum decreased over time, while Sargassum transported by the wind-driven ocean currents first increased and then decreased. Such changes in Sargassum amount over time are also observed in Fig. 3. Specifically, during May 10-16, 2014, the stationary cyclonic eddy (yellow circle in Fig. 3) in the Bay of Campeche was virtually free of Sargassum (Fig. 3a). After two weeks, the Sargassum amount increased sharply (Fig. 3b), and then declined gradually starting from June 5th (Fig. 3c & d).

Another example is when the main axis of the LCS had a northward position at ~26°N, where it can also significantly affect the spatial distribution patterns of Sargassum in different years (i.e., 2017, 2018, 2019; Fig. 5g-i) and in the same year (i.e., 2018; Fig. 5j-l). For the former cases, in both 2018 and 2019, more Sargassum was found than in 2017 in the northern part of the LCS (within the well-developed but still undetached LCE), when direct transport of Sargassum from the northwestern Caribbean Sea to the Straits of Florida also occurred (see the white curves with arrows in Fig. 5h & i). For the latter cases, between early June and late July of 2018, different locations/shapes of the LC and the undetached LCE led to different Sargassum transport and distribution patterns. During June 18-24 (Fig. 5k), the undetached LCE was oriented in the northwest-southeast direction, while it changed to the west-east direction during July 15-21 (Fig. 51) when the LC penetrated further north (at \sim 24°N). The distribution patterns of Sargassum closely followed these circulation patterns, which were dramatically different from those during June 7-13 (Fig. 5j).

In general, ocean surface currents and eddies in the GoM have strongly influenced the transport and spatial distribution patterns of *Sargassum*. In the adjacent Straits of Florida, where cyclonic eddy activity is intense (Kourafalou and Kang, 2012; Zhang et al., 2019), ocean eddies also contribute to *Sargassum* transport. As shown in Fig. 6, *Sargassum* entrained within a cyclonic eddy was transported eastward along the Florida Keys due to the eastward movement of the eddy.

4. Discussion

The observations above are based on the combined *Sargassum* and surface ocean current maps, with the *Sargassum* distribution patterns explained by physical transport mechanisms. Although local growth and

Table 1

Durations (number of days) of different transport pathways of Sargassum of Caribbean origin in the GoM, determined from "daily" Sargassum biomass density images (calculated as an average of the past seven days with the current day included) between January 2014 and June 2023. This analysis is focused on years after 2013, before which the Sargassum amount in the Caribbean Sea was minimal.

Mechanism year	Northward transport	Eastward transport	Westward transport (M-1)	Westward transport (M-2)	Westward transport (M-3)	Westward transport (M-4)	Westward transport (M-5)	Westward transport (M-6)
2014	127	73	53	0	40	0	41	0
2015	60	152	76	58	70	10	65	6
2016	0	0	0	0	0	0	0	0
2017	114	98	42	0	11	0	43	10
2018	159	196	152	68	98	10	87	8
2019	228	239	71	71	25	22	180	47
2020	68	75	67	51	23	9	27	0
2021	124	161	112	61	41	11	151	0
2022	172	197	143	84	93	41	170	25
2023	120	130	74	0	17	12	116	34

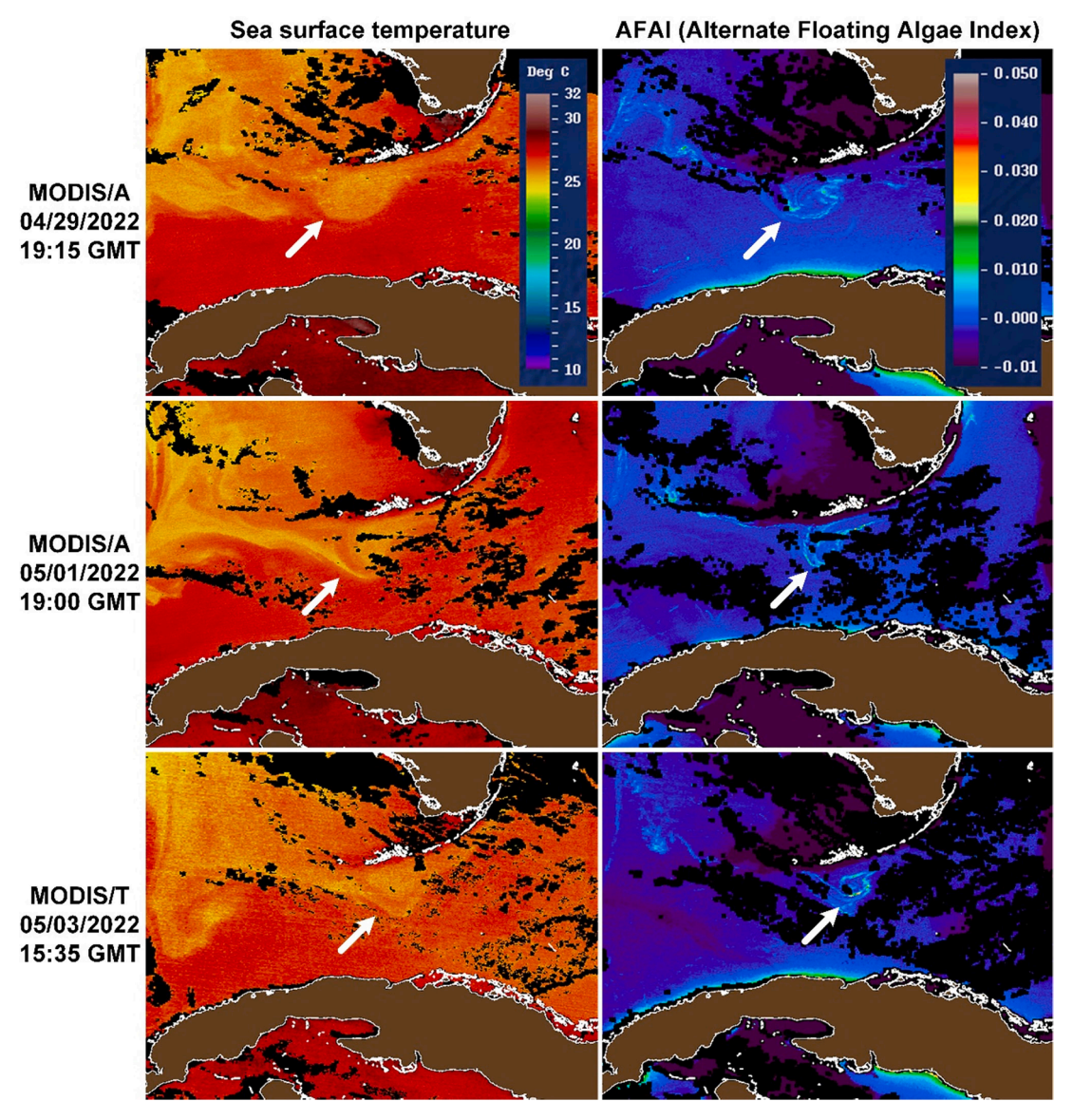


Fig. 6. Distributions of MODIS sea surface temperature (unit: °C; left panel) and Alternate Floating Algae Index (AFAI, no unit; right panel) in the Straits of Florida on April 29, May 1, and May 3, 2022, showing the eastward transport of *Sargassum* due to the eastward movement of a cyclonic eddy. The positions of the cyclonic eddy and related *Sargassum* rafts are indicated by white arrows. Black color in each image means no data. These images cover a region of 21.6°N–26°N and 84.5°W–79°W, and they were obtained from https://optics.marine.usf.edu/cgi-bin/optics_data?roi=GCOOS¤t=1.

mortality can also change *Sargassum* abundance and distribution without physical transport, local growth is unlikely to explain the temporal changes in specific locations in the cases examined above. For example, under typical conditions, *Sargassum* daily doubling rate was estimated to be ~ 0.03 (Wang et al., 2019). Then, in one week, local growth would lead to an increase of $(2^{(0.03\times7)}-1)=16$ %, and in two weeks the increased amount would be 34%, not sufficient to explain the much higher changes at fixed locations between sequential weekly images. Therefore, although local growth or mortality cannot be ruled out due to lack of in situ data, their roles in determining the spatial distribution patterns of *Sargassum* are likely minor as compared to physical transport.

It should be noted that the growth rate of Sargassum varies over time, and the method (e.g., in situ and ex-situ culture systems vs satellite observations) used to calculate the growth rate can also influence the results. In this study, the selected daily Sargassum doubling rate (\sim 0.03) is a mean growth rate, derived from satellite observations of Sargassum during Sargassum growing seasons (Wang et al., 2019), and it can be smaller than the growth rates derived from in situ and ex-situ culture

systems (e.g., ~0.03–0.06 from Magaña-Gallegos et al., 2023). In addition, we note that in many previous studies of pelagic *Sargassum* (e.g., Johns et al., 2020; Marsh et al., 2021), 1 % windage (i.e., 1 % of the 10 m winds; direct momentum transfer from the winds to floating materials) has been added to surface current velocity field to achieve better understanding of *Sargassum* transport and prediction. Here, 1 % windage for the GoM (equivalent to ~0.01–0.06 m/s; Zhang and Hu, 2021) is negligible compared to the strong ocean current field of the GoM (e.g., >0.5 m/s for the LC/FC system and LCEs, Liu et al., 2016 and Zhang et al., 2023; ~0.3–0.35 m/s for the ocean currents on the Campeche Bank, Lilly and Pérez-Brunius, 2021), therefore, windage effects were not considered in this study.

Similar to ocean currents, Stokes drift (residual transport due to ocean waves) can also contribute to the transport of drifting materials, particularly in shallow, nearshore waters (e.g., Monismith and Fong, 2004; Röhrs et al., 2012; Hunter et al., 2022), which induces a displacement of materials parallel to the direction of wave propagation (Jouanno et al., 2021). This mechanism allows *Sargassum* to migrate and possibly accumulate in shallow waters along the coasts. The Stokes drift

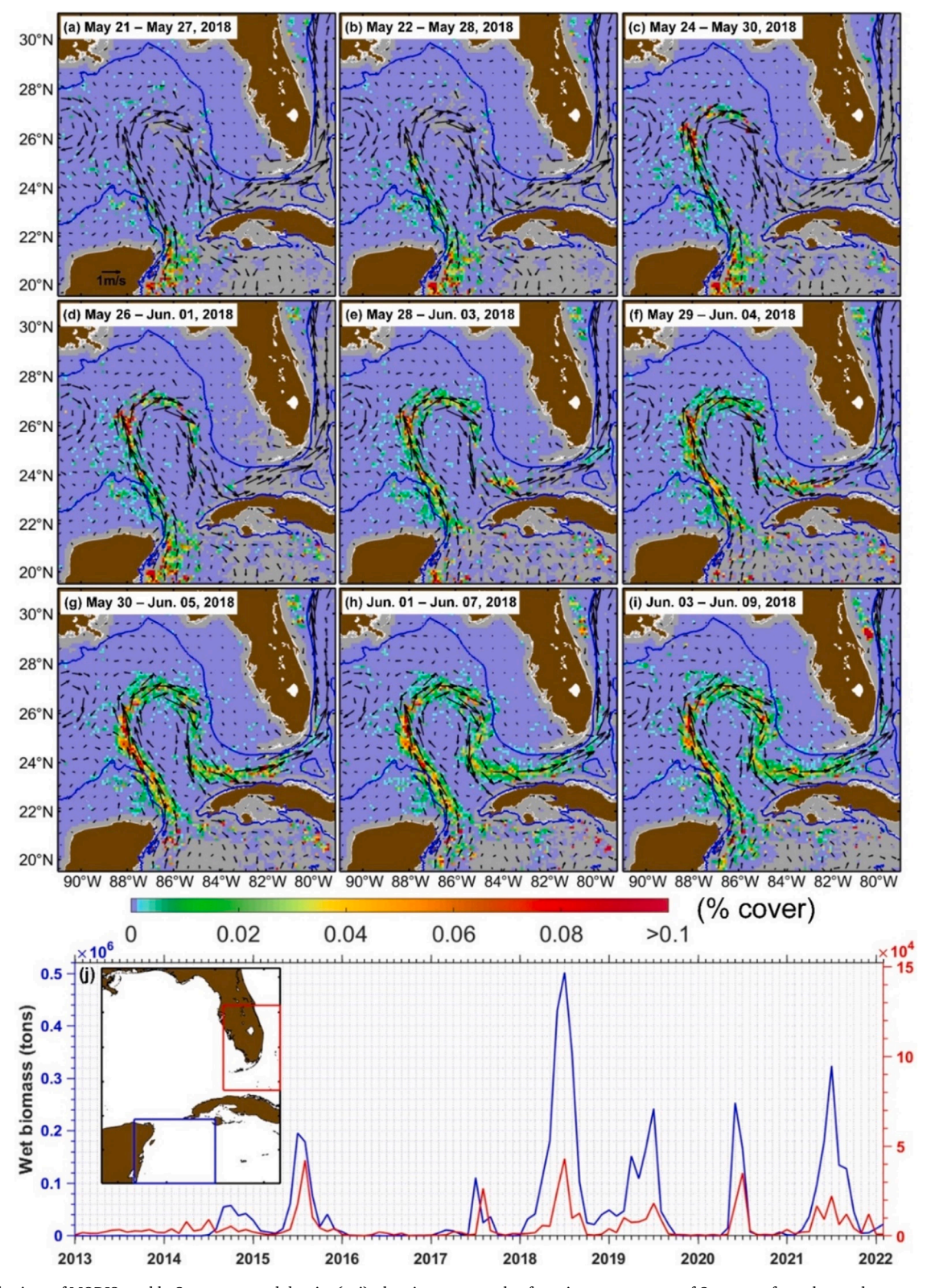


Fig. 7. Distributions of MODIS weekly *Sargassum* areal density (a–i), showing an example of continuous transport of *Sargassum* from the northwestern Caribbean Sea to the Straits of Florida. A value of 0.02 on the color bar denotes 0.02 %. Gray color indicates no data, and the blue lines represent the 200 m isobath in each figure. The black vectors in each figure (with scale shown in (a)) represent altimetry-based ocean surface currents. (j) shows the time series of wet biomass of *Sargassum* from the northwestern Caribbean Sea (blue color) and southeast coast of Florida (red color) between January 2013 and February 2022, and the year mark starts from January.

effects were not considered in this paper because 1) the focus of this study is on the transport of large amounts of pelagic *Sargassum* in the open GoM rather than in shallow nearshore waters where the influence

of ocean waves is more important, and 2) in the open GoM, surface current velocities are generally $\sim\!8\text{--}10$ times larger than Stokes drift velocities (Bosi et al., 2021). This omission is consistent with previous

studies focusing on the simulation and prediction of *Sargassum* transport in the tropical and subtropical North Atlantic (e.g., Brooks et al., 2018; Putman et al., 2018; Wang et al., 2019; Marsh et al., 2021). Nevertheless, future studies on *Sargassum* transport in shallow nearshore waters should consider the Stokes drift effects.

The findings above have significant implications on *Sargassum* forecasts for sensitive coastal habitats in Florida, where recurrent beaching events have been reported in the Florida Keys and along the east coast of Florida (e.g., Miami Beach and Palm Beach; Trinanes et al., 2021; Zhang et al., 2022a). For example, how long will it take to transport *Sargassum* from the northwestern Caribbean Sea, or from the northern edge of the LCS, to the Florida Keys and the east coast of Florida? Figs. 7a–7i show an example of continuous transport of *Sargassum* from the northwestern Caribbean Sea to the Florida Keys and east coast of Florida. From this image sequence, *Sargassum* reached the northern edge of the LC during May 24–30, 2018 (Fig. 7c) and was then transported to the Florida Keys in about 5 days (Fig. 7c–f). After about 3 more days, *Sargassum* reached the east coast of Florida near Miami (Fig. 7h). These results can be explained by the mean velocity of the LC/FC system (~1.2–1.6 m/s, Zhang et al., 2022b).

The transport can also be revealed through a lag analysis of time series of Sargassum wet biomass (as shown in Fig. 7j). For the period January 2013-February 2022, the two time series of the northwestern Caribbean Sea (blue color in Fig. 7j) and around the southeast coast of Florida (red color in Fig. 7j) suggest a one-month lag between the two, especially in the summer months of major Sargassum years of 2015, 2017, 2018, and 2020. The two exceptional years are 2019 and 2021, when Sargassum was transported to south Florida directly from the tropical Atlantic Ocean via the North Equatorial Current and the Antilles Current (Drouin et al., 2022), as observed from the SaWS (https://opti cs.marine.usf.edu/projects/saws.html). Another exception occurred in 2014, when Sargassum in the GoM appeared to have a local origin (as shown in Fig. 3). In all cases, the Sargassum amount in the latter region is not necessarily proportional to that in the former region, clearly indicating the complexity of Sargassum transport and growth. Note that the one-month lag described here is different from the number of days when the eastward transport of Sargassum was observed during a year (third column of Table 1): the former is directly relevant to the behavior and velocity of the LC/FC system, while the latter indicates the duration of such an eastward transport.

Finally, our findings on the Sargassum transport in the GoM were made possible not only by the availability of advanced satellite-based Sargassum products, but also by the full use of ocean surface current products derived from multiple altimeters. The method used in this study can be extended to other relevant topics, such as marine debris and spilled oil transport (e.g., Liu et al., 2011; Kourafalou and Androulidakis, 2013; Jolliff et al., 2014; Abascal et al., 2015; Weisberg et al., 2011, 2017). Indeed, the transport mechanisms of GoM Sargassum introduced in this study represent the dominant mechanisms responsible for the transport of large amounts of Sargassum in the GoM, which were derived from the combined maps of Sargassum areal density (0.1 $^{\circ}$ × 0.1 $^{\circ}$) and altimetry-based surface geostrophic currents (0.25 $^{\circ}$ \times 0.25 $^{\circ}$). The transport mechanisms of GoM Sargassum at smaller scale may have been overlooked here, and the Sargassum transport mechanisms over the coastal areas (e.g., the West Florida Shelf and Louisiana-Texas Shelf) may have not be fully revealed due to the deficiencies in current satellite altimetry products. However, these limitations may be overcome with the availability of novel surface current products at higher spatial resolution from more advanced satellite altimetry missions (e.g., Surface Water and Ocean Topography or SWOT; https://swot.jpl.nasa.gov/). Moreover, in addition to surface currents, reliable data on local winds, waves, and tides are also essential in interpreting Sargassum beaching in nearshore coastal waters. In such environments, the processes elucidating how Sargassum detaches from major surface currents remain unknown and therefore should be investigated in future research.

5. Conclusions

Based on satellite observations of Sargassum areal density and ocean surface currents, we have shown that large amounts of Sargassum in the GoM can either originate from the northwestern GoM or be a result of physical transport from the northwestern Caribbean Sea, each having their specific transport pathways that influence the spatial distribution patterns of this brown seaweed. The LCS and associated eddies were found to play a key role in the Sargassum transport within the GoM. Time series analysis also revealed that Sargassum along the southeast coast of Florida may lag Sargassum in the northwestern Caribbean Sea by about one month in most years with major Sargassum blooms, all under the influence of the Great Atlantic Sargassum Belt.

Supporting Information

The animation showing the eastward transport of *Sargassum* from the northwestern GoM to the eastern GoM can be accessed at:https://optics.marine.usf.edu/projects/GoM_Sargassum_transport/NW_GoM_Sargassum_eastward_transport.html

The animation showing the westward transport of <code>Sargassum</code> controlled by mechanism 4 (i.e., relaying of ocean eddies) and mechanism 6 (i.e., westward transport of the westward ocean currents with/without currents associated with eddies in the northern/central GoM) can be accessed at:https://optics.marine.usf.edu/projects/GoM_Sargassum_transport/GoM_Sargassum_westward_transport_animation.html

CRediT authorship contribution statement

Yingjun Zhang: Data curation, Formal analysis, Investigation, Methodology, Writing – original draft, Writing – review & editing. Chuanmin Hu: Conceptualization, Funding acquisition, Investigation, Methodology, Project administration, Resources, Supervision, Visualization, Writing – original draft, Writing – review & editing. Dennis J. McGillicuddy: Investigation, Visualization, Writing – original draft, Writing – review & editing. Brian B. Barnes: Funding acquisition, Investigation, Methodology, Writing – original draft, Writing – review & editing. Yonggang Liu: Investigation, Methodology, Writing – original draft, Writing – review & editing. Vassiliki H. Kourafalou: Investigation, Writing – original draft, Writing – original draft. Frank J. Hernandez: Investigation, Project administration, Writing – original draft, Writing – review & editing.

Declaration of competing interest

The authors declare that they have no known competing financial interests or personal relationships that could have appeared to influence the work reported in this paper.

Data availability

The data products used in this study are publicly available. Weekly <code>Sargassum</code> areal density data products were generated and distributed through the <code>Sargassum</code> Watch System (SaWS, https://optics.marine.usf.edu/projects/saws.html) by the Optical Oceanography Laboratory at the University of South Florida. The altimetry data products were obtained from the Copernicus Marine Environment Monitoring Service (https://doi.org/10.48670/moi-00148).

Acknowledgements

This work was supported by the NASA student fellowship program "Future Investigators in NASA Earth and Space Science and Technology"

(FINESST, 80NSSC19K1358), NASA Ocean Biology and Biogeochemistry program (80NSSC20M0264), NASA Biodiversity and Ecological Forecasting program (80NSSC21K0422), NOAA NCCOS MERHAB program (NA23NOS4780291), EPA South Florida program (02D42923), National Academy of Sciences Gulf Research Program (SCON-10000542), NOAA RESTORE Science Program (NA17NOS4510099), National Science Foundation (OCE-1840381), National Institute of Environmental Health Sciences (1P01ES028938), and the Isham Family Charitable Fund. We thank the two anonymous reviewers for their constructive comments and suggestions to improve the presentation of this work.

References

- Abascal, A.J., Castanedo, S., Minguez, R., Medina, R., Liu, Y., Weisberg, R.H., 2015. Stochastic Lagrangian trajectory modeling of surface drifters deployed during the Deepwater Horizon oil spill. In: Proc. 38th AMOP Tech. Seminar Env. Contamination & Response, Env. & Climate Change Canada, Ottawa, ON, pp. 71–99.
- Alvera-Azcárate, A., Barth, A., Weisberg, R.H., 2009. The surface circulation of the Caribbean Sea and the Gulf of Mexico as inferred from satellite altimetry. J. Phys. Oceanogr. 39 (3), 640–657. https://doi.org/10.1175/2008JPO3765.1.
- Amador-Castro, F., García-Cayuela, T., Alper, H.S., Rodriguez-Martinez, V., Carrillo-Nieves, D., 2021. Valorization of pelagic *Sargassum* biomass into sustainable applications: current trends and challenges. J. Environ. Manage. 283, 112013 https://doi.org/10.1016/j.jenvman.2021.112013.
- Andrade-Canto, F., Beron-Vera, F.J., Goni, G.J., Karrasch, D., Olascoaga, M.J., Triñanes, J., 2022. Carriers of *Sargassum* and mechanism for coastal inundation in the Caribbean Sea. Phys. Fluids 34 (1), 016602. https://doi.org/10.1063/ 5.0079055.
- Brooks, M.T., Coles, V.J., Hood, R.R., Gower, J.F., 2018. Factors controlling the seasonal distribution of pelagic *Sargassum*. Mar. Ecol. Prog. Ser. 599, 1–18. https://doi.org/ 10.3354/meps12646.
- Bosi, S., Broström, G., Roquet, F., 2021. The role of Stokes drift in the dispersal of North Atlantic surface marine debris. Front. Mar. Sci. 8, 697430 https://doi.org/10.3389/ fmars.2021.697430.
- Casazza, T.L., Ross, S.W., 2008. Fishes associated with pelagic Sargassum and open water lacking Sargassum in the Gulf Stream of North Carolina. Fishery Bull. 106 (4), 348–363
- Chen, Y., 2017. Fish resources of the Gulf of Mexico. In: Ward, C. (Ed.), Habitats and Biota of the Gulf of Mexico: Before the Deepwater Horizon Oil Spill. Springer. https://doi.org/10.1007/978-1-4939-3456-0_1.
- Doyle, E., Franks, J., 2015. Sargassum Fact Sheet. Gulf and Caribbean Fisheries Institute, p. 4 pp.
- Drouin, K.L., Lozier, M.S., Beron-Vera, F.J., Miron, P., Olascoaga, M.J., 2022. Surface pathways connecting the South and North Atlantic oceans. Geophys. Res. Lett. 49, e2021GL096646 https://doi.org/10.1029/2021GL096646.
- Elliott, B.A., 1982. Anticyclonic rings in the Gulf of Mexico. J. Phys. Oceanogr. 12 (11), 1292–1309. https://doi.org/10.1175/1520-0485(1982)012≤1292:ARITGO≥2.0. CO: 2.
- Felder, D.L., Camp, D.K. and Tunnel, W., Jr., 2009. An introduction to Gulf of Mexico biodiversity assessment. In D.L. Felder and D.K. Camp (Eds.), Gulf of Mexico Origin, Waters, and Biota, Volume 1, Biodiversity. Texas A & M University Press.
- Franks, J.S., Johnson, D.R., Ko, D.S., 2016. Pelagic *Sargassum* in the tropical North Atlantic. Gulf Caribbean Res 27 (1), SC6–SC11. https://doi.org/10.18785/
- Gower, J., Hu, C., Borstad, G., King, S., 2006. Ocean color satellites show extensive lines of floating *Sargassum* in the Gulf of Mexico. IEEE Trans. Geosci. Remote Sens. 44, 3619–3625. https://doi.org/10.1109/TGRS.2006.882258.
- Gower, J., King, S., 2011. Distribution of floating Sargassum in the Gulf of Mexico and the Atlantic ocean mapped using MERIS. Int. J. Remote Sens. 32, 1917–1929. https://doi.org/10.1080/01431161003639660.
- Gower, J., Young, E., King, S., 2013. Satellite images suggest a new Sargassum source region in 2011. Remote Sens. Lett. 4 (8), 764–773. https://doi.org/10.1080/ 2150704X.2013.796433.
- Gower, J., King, S., 2019. Seaweed, seaweed everywhere. Science 365 (6448). https://doi.org/10.1126/science.aay0989, 27-27.
- Gower, J., King, S., 2020. The distribution of pelagic *Sargassum* observed with OLCI. Int. J. Remote Sens. 41 (15), 5669–5679. https://doi.org/10.1080/ 01431161.2019.1658240.
- Hamilton, P., Fargion, G.S., Biggs, D.C., 1999. Loop current eddy paths in the western Gulf of Mexico. J. Phys. Oceanogr. 29 (6), 1180–1207. https://doi.org/10.1175/1520-0485(1999)029<1180-1.CEPIT>2.0.CO:2.
- Hu, C., Cannizzaro, J., Carder, K.L., Muller-Karger, F.E., Hardy, R., 2010. Remote detection of Trichodesmium blooms in optically complex coastal waters: examples with MODIS full-spectral data. Remote Sens. Environ. 114 (9), 2048–2058. https:// doi.org/10.1016/j.rse.2010.04.011.
- Hu, C., Hardy, R., Ruder, E., Geggel, A., Feng, L., Powers, S., Hernandez, F., Graettinger, G., Bodnar, J., McDonald, T., 2016a. Sargassum coverage in the northeastern Gulf of Mexico during 2010 from Landsat and airborne observations: implications for the Deepwater Horizon oil spill impact assessment. Mar. Pollut. Bull. 107 (1), 15–21. https://doi.org/10.1016/j.marpolbul.2016.04.045.

Hu, C., Murch, B., Barnes, B.B., Wang, M., Maréchal, J.P., Franks, J., Johnson, D., Lapointe, B.E., Goodwin, D.S., Schell, J.M., Siuda, A.N.S., 2016b. Sargassum watch warns of incoming seaweed. Eos (Washington DC) 97, 10–15. https://doi.org/ 10.1029/2016F0058355

- Hu, C., Wang, M., Lapointe, B.E., Brewton, R.A., Hernandez, F.J., 2021. On the Atlantic pelagic Sargassum's role in carbon fixation and sequestration. Sci. Total Environ. 781, 146801 https://doi.org/10.1016/j.scitoteny.2021.146801.
- Hunter, E.J., Fuchs, H.L., Wilkin, J.L., Gerbi, G.P., Chant, R.J., Garwood, J.C., 2022. ROMSPath v1. 0: offline particle tracking for the regional ocean modeling system (ROMS). Geosci. Model Dev. 15 (11), 4297–4311. https://doi.org/10.5194/gmd-15-4297-2022
- Johns, E.M., Lumpkin, R., Putman, N.F., Smith, R.H., Muller-Karger, F.E., Rueda-Roa, D. T., Hu, C., Wang, M., Brooks, M.T., Gramer, L.J., Werner, F.E., 2020. The establishment of a pelagic Sargassum population in the tropical Atlantic: biological consequences of a basin-scale long distance dispersal event. Prog. Oceanogr. 182, 102269 https://doi.org/10.1016/j.pocean.2020.102269.
- Jolliff, J.K., Smith, T.A., Ladner, S., Arnone, R.A., 2014. Simulating surface oil transport during the Deepwater Horizon oil spill: experiments with the BioCast system. Ocean Modell. 75, 84–99. https://doi.org/10.1016/j.ocemod.2014.01.004.
- Jouanno, J., Benshila, R., Berline, L., Soulié, A., Radenac, M.H., Morvan, G., Diaz, F., Sheinbaum, J., Chevalier, C., Thibaut, T., Changeux, T., 2021. A NEMO-based model of *Sargassum* distribution in the tropical Atlantic: description of the model and sensitivity analysis (NEMO-Sarg1.0). Geosci. Model Dev. 14 (6), 4069–4086. https:// doi.org/10.5194/gmd-14-4069-2021.
- Kourafalou, V.H., Kang, H., 2012. Florida Current meandering and evolution of cyclonic eddies along the Florida Keys Reef Tract: are they interconnected? J. Geophys. Res.: Oceans 117. https://doi.org/10.1029/2011JC007383. C05028.
- Kourafalou, V.H., Androulidakis, Y.S., 2013. Influence of Mississippi River induced circulation on the Deepwater Horizon oil spill transport. J. Geophys. Res. Ocean. 118, 3823–3842. https://doi.org/10.1002/jgrc.20272.
- Lapointe, B.E., Brewton, R.A., Herren, L.W., Wang, M., Hu, C., McGillicuddy Jr, D.J., Lindell, S., Hernandez, F.J., Morton, P.L., 2021. Nutrient content and stoichiometry of pelagic Sargassum reflects increasing nitrogen availability in the Atlantic Basin. Nat. Commun. 12 (1), 3060. https://doi.org/10.1038/s41467-021-23135-7.
- Leben, R.R., 2005. Altimeter-derived loop current metrics. In Circulation in the Gulf of Mexico: Observations and Models (eds W. Sturges and A. Lugo & #8208; Fernandez). https://doi.org/10.1029/161GM15.
- Le Hénaff, M., Kourafalou, V.H., 2016. Mississippi waters reaching South Florida reefs under no flood conditions: synthesis of observing and modeling system findings. Ocean Dyn. 66 (3), 435–459. https://doi.org/10.1007/s10236-016-0932-4.
- Lilly, J.M., Pérez-Brunius, P., 2021. A gridded surface current product for the Gulf of Mexico from consolidated drifter measurements. Earth Syst. Sci. Data 13 (2), 645–669. https://doi.org/10.5194/essd-13-645-2021.
- Liu, Y., Weisberg, R.H., Hu, C., Zheng, L., 2011. Tracking the Deepwater Horizon oil spill: a modeling perspective. Eos, Trans. Am. Geophys. Union 92 (6), 45–46. https://doi. org/10.1029/2011E0060001.
- Liu, Y., Weisberg, R.H., Vignudelli, S., Mitchum, G.T., 2014. Evaluation of altimetry-derived surface current products using Lagrangian drifter trajectories in the eastern Gulf of Mexico. Journal of Geophysical Research Oceans 119, 2827–2842. https://doi.org/10.1002/20131C009710
- Liu, Y., Weisberg, R.H., Vignudelli, S., Mitchum, G.T., 2016. Patterns of the loop current system and regions of sea surface height variability in the eastern Gulf of Mexico revealed by the self-organizing maps. J. Geophys. Res.: Oceans 121 (4), 2347–2366. https://doi.org/10.1002/2015JC011493.
- Magaña-Gallegos, E., García-Sánchez, M., Graham, C., Olivos-Ortiz, A., Siuda, A.N., van Tussenbroek, B.I., 2023. Growth rates of pelagic Sargassum species in the Mexican Caribbean. Aquat. Bot. 185, 103614 https://doi.org/10.1016/j. aquiabrt 2022 103614
- Marsh, R., Addo, K.A., Jayson-Quashigah, P.N., Oxenford, H.A., Maxam, A., Anderson, R., Skliris, N., Dash, J., Tompkins, E.L., 2021. Seasonal predictions of holopelagic Sargassum across the tropical Atlantic accounting for uncertainty in drivers and processes: the SARTRAC ensemble forecast system. Front. Mar. Sci. 8, 722524 https://doi.org/10.3389/fmars.2021.722524.
- Martin, L.M., Taylor, M., Huston, G., Goodwin, D.S., Schell, J.M., Siuda, A.N., 2021.
 Pelagic Sargassum morphotypes support different rafting motile epifauna communities. Mar. Biol. 168, 1–17. https://doi.org/10.1007/s00227-021-03910-2.
- McGillicuddy Jr, D.J., Morton, P.L., Brewton, R.A., Hu, C., Kelly, T.B., Solow, A.R., Lapointe, B.E., 2023. Nutrient and arsenic biogeochemistry of Sargassum in the western Atlantic. Nat. Commun. 14 (1), 6205. https://doi.org/10.1038/s41467-023-
- Milledge, J.J., Nielsen, B.V., Bailey, D., 2016. High-value products from macroalgae: the potential uses of the invasive brown seaweed, *Sargassum* muticum. Rev. Environ. Sci. Bio/Technol. 15 (1), 67–88. https://doi.org/10.1007/s11157-015-9381-7.
- Monismith, S.G., Fong, D.A., 2004. A note on the potential transport of scalars and organisms by surface waves. Limnol. Oceanogr. 49 (4), 1214–1217. https://doi.org/ 10.4319/lo.2004.49.4.1214.
- Orozco-González, J.G., Amador-Castro, F., Gordillo-Sierra, A.R., García-Cayuela, T., Alper, H.S., Carrillo-Nieves, D., 2022. Opportunities surrounding the use of *Sargassum* biomass as precursor of biogas, bioethanol, and biodiesel production. Front. Mar. Sci. 8, 791054 https://doi.org/10.3389/fmars.2021.791054.
- Putman, N.F., Goni, G.J., Gramer, L.J., Hu, C., Johns, E.M., Trinanes, J., Wang, M., 2018. Simulating transport pathways of pelagic *Sargassum* from the equatorial Atlantic into the Caribbean Sea. Prog. Oceanogr. 165, 205–214. https://doi.org/10.1016/j. pocean.2018.06.009.
- Qi, L., Hu, C., Mikelsons, K., Wang, M., Lance, V., Sun, S., Barnes, B.B., Zhao, J., Van der Zande, D., 2020. In search of floating algae and other organisms in global oceans and

- lakes. Remote Sens. Environ. 239, 111659 https://doi.org/10.1016/j.
- Richardson, P.L., 2005. Caribbean current and eddies as observed by surface drifters.

 Deep Sea Res. Part II: Top. Stud. Oceanogr. 52 (3–4), 429–463. https://doi.org/10.1016/j.dsr2.2004.11.001.
- Röhrs, J., Christensen, K.H., Hole, L.R., Broström, G., Drivdal, M., Sundby, S., 2012. Observation-based evaluation of surface wave effects on currents and trajectory forecasts. Ocean Dyn. 62, 1519–1533. https://doi.org/10.1007/s10236-012-0576-y.
- Sanchez-Rubio, G., Perry, H., Franks, J.S., Johnson, D.R., 2018. Occurrence of pelagic Sargassum in waters of the U.S. Gulf of Mexico in response to weather-related hydrographic regimes associated with decadal and interannual variability in global climate. Fishery Bull. 116 (1), p93–106. https://doi.org/10.7755/FB.116.1.10.
- Schmitz Jr., W.J., 2005. Cyclones and westward propagation in the shedding of anticyclonic rings from the loop current. In: Sturges, W., Lugo, A. (Eds.), Circulation in the Gulf of Mexico: Observations and Models. Fernandez. https://doi.org/ 10.1029/161GM18. #8208.
- Siuda, A.N., Schell, J.M., Goodwin, D.S., 2016. Unprecedented proliferation of novel pelagic Sargassum form has implications for ecosystem function and regional diversity in the Caribbean. In: Ocean Sciences Meeting 2016. American Geophysical Union, pp. ME14E–M0682.
- Smetacek, V., Zingone, A., 2013. Green and golden seaweed tides on the rise. Nature 504 (7478), 84–88. https://doi.org/10.1038/nature12860.
- Trinanes, J., Putman, N.F., Goni, G., Hu, C., Wang, M., 2021. Monitoring pelagic Sargassum inundation potential for coastal communities. J. Oper. Oceanogr. 1–12. https://doi.org/10.1080/1755876X.2021.1902682.
- Van Sebille, E., Zettler, E., Wienders, N., Amaral-Zettler, L., Elipot, S., Lumpkin, R., 2021. Dispersion of surface drifters in the tropical Atlantic. Front. Mar. Sci. 7, 607426 https://doi.org/10.3389/fmars.2020.607426.
- Van Tussenbroek, B.I., Arana, H.A.H., Rodríguez-Martínez, R.E., Espinoza-Avalos, J., Canizales-Flores, H.M., González-Godoy, C.E., Barba-Santos, M.G., Vega-Zepeda, A., Collado-Vides, L., 2017. Severe impacts of brown tides caused by Sargassum spp. on near-shore Caribbean seagrass communities. Mar. Pollut. Bull. 122 (1–2), 272–281. https://doi.org/10.1016/j.marpolbul.2017.06.057.
- Vignudelli, S., Snaith, H.M., Lyard, F., Cipollini, P., Venuti, F., Birol, F., Bouffard, J., Roblou, L., 2006. Satellite radar altimetry from open ocean to coasts: challenges and perspectives. Remote Sens. Mar. Environ. 6406, 148–159. https://doi.org/10.1117/ 12.694024.
- Wang, M., Hu, C., 2016. Mapping and quantifying Sargassum distribution and coverage in the Central West Atlantic using MODIS observations. Remote Sens. Environ. 183, 350–367. https://doi.org/10.1016/j.rse.2016.04.019.
- Wang, M., Hu, C., 2017. Predicting Sargassum blooms in the Caribbean Sea from MODIS observations. Geophys. Res. Lett. 44 (7), 3265–3273. https://doi.org/10.1002/2017G1072932
- Wang, M., Hu, C., Cannizzaro, J., English, D., Han, X., Naar, D., Lapointe, B., Brewton, R., Hernandez, F., 2018. Remote sensing of *Sargassum* biomass, nutrients, and pigments. Geophys. Res. Lett. 45 (22), 12–359. https://doi.org/10.1029/2018GL078858.
- Wang, M., Hu, C., Barnes, B.B., Mitchum, G., Lapointe, B., Montoya, J.P., 2019. The great Atlantic Sargassum belt. Science 365 (6448), 83–87. https://doi.org/10.1126/ science.aaw7912.

- Webster, R.K., Linton, T., 2013. Development and implementation of *Sargassum* early advisory system (SEAS). Shore Beach 81 (3), 1.
- Weisberg, R.H., Zheng, L., Liu, Y., 2011. Tracking subsurface oil in the aftermath of the Deepwater Horizon well blowout. In: Liu, Y., MacFadyen, A., Ji, Z.-G., Weisberg, R. H. (Eds.), Monitoring and Modeling the Deepwater Horizon Oil Spill: A Record-Breaking Enterprise, 195. Geophys. Monogr. Ser, pp. 205–215. https://doi.org/ 10.1029/2011GM001131. Washington, DC: The American Geophysical Union).
- Weisberg, R.H., Zheng, L., Liu, Y., Murawski, S., Hu, C., Paul, J., 2016. Did Deepwater Horizon hydrocarbons transit to the west Florida continental shelf? Deep Sea Res. Part II: Topic. Stud. Oceanogr. 129, 259–272. https://doi.org/10.1016/j. dsr2.2014.02.002.
- Weisberg, R.H., Zheng, L., Liu, Y., 2017. On the movement of Deepwater horizon oil to northern gulf beaches. Ocean Modelling 111, 81–97. https://doi.org/10.1016/j. ocemod.2017.02.002.
- Wells, R.J., Rooker, J.R., 2004. Spatial and temporal patterns of habitat use by fishes associated with *Sargassum* mats in the northwestern Gulf of Mexico. Bull. Mar. Sci. 74 (1), 81–99.
- Witherington, B., Hirama, S., Hardy, R., 2012. Young sea turtles of the pelagic Sargassum-dominated drift community: habitat use, population density, and threats. Mar. Ecol. Prog. Ser. 463, 1–22. https://doi.org/10.3354/meps09970.
- Zavala-Hidalgo, J., Romero-Centeno, R., Mateos-Jasso, A., Morey, S.L., Martínez-López, B., 2014. The response of the Gulf of Mexico to wind and heat flux forcing: what has been learned in recent years? Atmósfera 27 (3), 317–334. https://doi.org/ 10.1016/s0187-6236(14)71119-1.
- Zhang, S., Hu, C., Barnes, B.B., Harrison, T.N., 2022a. Monitoring Sargassum Inundation on Beaches and Nearshore Waters Using PlanetScope/Dove Observations. IEEE Geoscience and Remote Sensing Letters 19, 1–5. https://doi.org/10.1109/ LGRS 2022 3148684
- Zhang, Y., Hu, C., Liu, Y., Weisberg, R.H., Kourafalou, V.H., 2019. Submesoscale and mesoscale eddies in the Florida straits: observations from satellite ocean color measurements. Geophys. Res. Lett. 46, 13262–13270. https://doi.org/10.1029/ 2019GL083999.
- Zhang, Y., Hu, C., 2021. Ocean temperature and color frontal zones in the Gulf of Mexico: where, when, and why. J. Geophys. Res.: Ocean. 126, e2021JC017544 https://doi. org/10.1029/2021JC017544.
- Zhang, Y., Hu, C., Kourafalou, V.H., Liu, Y., McGillicuddy, D.J., Barnes, B.B., Hummon, J. M., 2022b. Physical characteristics and evolution of a long-lasting mesoscale cyclonic eddy in the Straits of Florida. Front. Mar. Sci. 9, 779450 https://doi.org/10.3389/fmars.2022.779450
- Zhang, Y., Hu, C., Barnes, B.B., Liu, Y., Kourafalou, V.H., McGillicuddy, D.J., et al., 2023. Bio-optical, physical, and chemical properties of a loop current Eddy in the Gulf of Mexico. J. Geophys. Res.: Oceans 128, e2022JC018726. https://doi.org/10.1029/ 2022JC018726.
- Zhu, Y., Liang, X., 2020. Coupling of the surface and near-bottom currents in the Gulf of Mexico. J. Geophys. Res.: Oceans 125, e2020JC016488. https://doi.org/10.1029/ 2020JC016488.